March 2018

Experimental investigation of blade and propeller loads during straight ahead sailing

Fabrizio ORTOLANI [a,1], Giulio DUBBIOSO [a], Ivan SANTIC [a] and Salvatore MAURO [a]

[a] *CNR-INSEAN, Via di Vallerano 139, 00128, Rome*

Abstract. During operative scenarios, the propeller can experience an inflow substantially different from the one considered in the design phases and the 3D character of the flow gives onset to a complete system of loads. The quantification of these loads is of paramount importance to assess the reliability of mechanical structures, the comfort on-board due to vibrations and the effects on the dynamic response of the vessel. In this work, a novel set up that allows to monitor the loads developed by a single blade was implemented on a free running, self propelled maneuvering model with the aim to investigate in details the performance of the propeller during realistic operative conditions. This preliminary work introduces the experimental set up and provides a preliminary overview of the results relative to straight ahead motion.

Keywords. blade loads measurements, propeller bearing loads, free running model tests, advanced ship model testing

1. Introduction

The thorough analysis of the bearing loads induced on the hull structure and the components of the propulsion system by the propeller relies on the quantification of the cyclic blade loads. Accurate and detailed analysis can nowadays be performed by computational techniques based on potential based solvers like Vortex Lattice or Boundary Elements Methods (VLM and BEM) or viscous solvers based on the solution of the averaged form of the Navier-Stokes equations (RANSE). These tools are extensively validated for propeller operating in typical design conditions in rectilinear motion; in these circumstances, the blade operates at its maximum efficiency and the flow (not considering the cavitation phenomena) is attached over the largest portions of the blades. On the other hand, in realistic or off-design conditions like motion in waves, maneuvering and stopping/acceleration, high incidences can be experienced at the blade sections causing the increase of thrust and torque and the generation of relevant in-plane forces and moments. In recent years the off-design performance of the propeller is appealing the research interest because novel criteria and stringent constraints are imposed in new design

[1]Corresponding Author: Fabrizio Ortolani, CNR-INSEAN, Via di Vallerano 139, 00128, Rome; E-mail:fabrizio.ortolani@cnr.it

for continuity of operation and safety at sea, low impact and pollution to the environment and on-board comfort. In off–design conditions, theoretical and numerical tools used in traditional design still need validation and verification; potential based solvers, although computationally efficient, may be inaccurate in evaluating the effect of flow separations on blade/propeller loads. Although viscous solvers overcome these drawbacks some way and the computation of the flow of a rotating propeller past a ship is nowadays affordable, this approach is still computationally demanding and, hence, prohibitive for a routine application during the design. On these basis, experimental activities and the development of non-standard set-up play a fundamental role to the understanding and quantification of the propeller loads operating in realistic and off-design conditions. Last but not least, accurate experimental data are necessary for the validation of numerical/theoretical propeller models. A new experimental setup for the evaluation of propeller radial loads in realistic operative conditions has been recently developed by means of a novel patented transducer able to measure propeller in-plane and bearing loads ([1], [2]). That activity evidenced interesting hydrodynamic phenomena that occur during the first phase of manoeuvres, giving rise to large radial loads that affect propeller performance, ship navigational behaviour and the mechanical stresses distributions along the shaft line, by means of free running maneuvering model tests ([1], [2]). The successive numerical analysis ([3], [4]) explained the relation between the character of the wake with the propeller developed loads and the central role played by propeller wake interactions during mild maneuvering conditions. This activity inspired the authors to move a further step in ship model testing with the aim to characterize single blade forces and integrated propeller loads in different operating conditions. In particular, the new set up has been implemented on a twin screw model and extensively tested at the CNR outdoor maneuvering basin at the Nemi lake. The present activity is one of the few attempts documented in literature for the monitoring of the complete blade/propeller system of loads by a free running maneuvering model. In the present paper the experimental set-up is described and the results obtained in rectilinear motion (approach phase of the maneuver) are discussed in terms of blade/propeller loads and their character is qualitatively explained referring to a generic wake of a twin screw ship.

2. Experimental Set Up

The experimental activity were performed at the CNR-INSEAN outdoor manoeuvring basin located at the Nemi lake. The selected unit is a 1 : 25 scaled model of a fast twin screw/twin rudder ship; the principal geometric characteristics of the model and the propeller are reported in table 1. The model is equipped with the standard instrumentation adopted in free running maneuvering model tests. In particular, each shaft line is moved by a brushless motor and an encoder to measure the rotational speed and angle; a diesel electric generator provides energy for all on-board instruments. The novelty regards the arrangement of one shaft-line equipped with a custom made instrumented propeller, to measure the complete system of loads (3 forces and 3 moments) acting on a single blade.

The propeller has been designed to house a commercial 6 components transducer, supporting one of the blades. Power supply and signal from transducer channels are transmitted to the acquisition system through high quality, low noise and low resistance, slip rings. A standard dynamometer measures thrust and torque on the same shaft.

Figure 1. Propeller and stern shell detail

B/T	3.9
L/B	6.9
C_B	0.46
D_{PROP} [m]	0.19
A_E/A_O	0.672
P/D	1.45
$N.\ Blades$	5

Table 1. Geometric details

3. Data Analysis

The complete system of loads provided by the transducer is referred to the frame that rotates with the blade; this frame is defined $B-frame$. To obtain the propeller loads (acting on the hub), a fixed frame of reference is introduced, namely the $H-frame$. The two frames are sketched in figure 2 and subscript "B" and "H" are introduced to distinguish the quantities in the two frames.

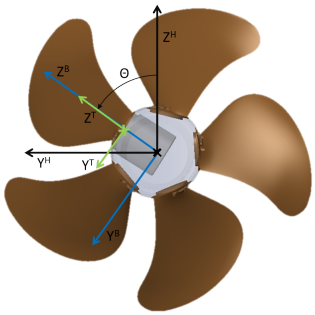

Figure 2. Reference frame

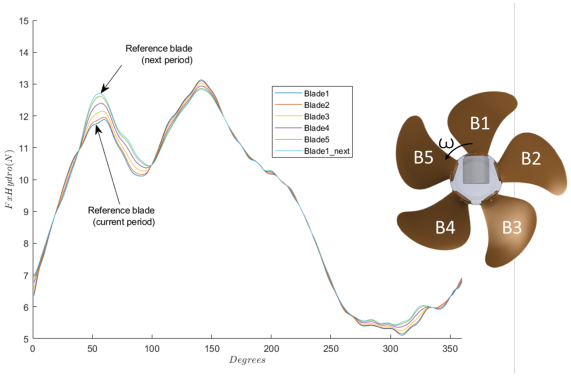

Figure 3. Propeller loads reconstruction

The loads in the $H-frame$ are obtained from the loads in the rotating frame by the following transformations:

$$F_x^H = F_x^B; \tag{1}$$

$$\begin{bmatrix} F_y^H \\ F_z^H \end{bmatrix} = \begin{bmatrix} cos(\Theta) & sin(\Theta) \\ -sin(\Theta) & cos(\Theta) \end{bmatrix} \begin{bmatrix} F_y^B \\ F_z^B \end{bmatrix}; \qquad \begin{bmatrix} M_y^H \\ M_z{}^H \end{bmatrix} = \begin{bmatrix} cos(\Theta) & sin(\Theta) \\ -sin(\Theta) & cos(\Theta) \end{bmatrix} \begin{bmatrix} M_y^B \\ M_z{}^B \end{bmatrix} \tag{2}$$

where Θ is the angular position of the blade with respect to z_H.

The data of a single run (maneuver) were collected according to the kinematic state of the model, that, in turn, corresponds to a different inflow to the propellers. For example, a turning circle maneuver is characterized by four phases, namely: the approach (rectilinear motion), the transient after the activation of the rudder, the stabilized phase and the pull–out (the rudder is moved to the neutral position).

In order to make the data consistent in terms of blade angle for all the cycles (propeller revolution), the measurements were re–sampled at steps of $1^\circ$and sliced for each period. The re–sampling of the data is considered to be useful for analyzing transient phases where discrepancies of the quantities can be expected for consecutive cycles.

The reconstruction of the total propeller loads from the single blade measurements has been obtained by a two–step procedure that accounts for the eventual variation of the inflow to the propeller and the geometric shift of the blades. In the first step, the load of the i–blade is derived from the signals of two consecutive cycles of the reference blade, as schematically described in figure 3: the new value at the generic position Θ is obtained from the first cycle by a linear increment that is proportional to the total variation between the two cycles:

$$F_i(\Theta) = F_{1cyc}(\Theta) + (F_{2cyc}(\Theta) - F_{1cyc}(\Theta))\,\frac{i-1}{Z} \tag{3}$$

where F_{1cyc} and F_{2cyc} are the signals of the two cycles, i is the actual blade and Z is the blade number. It is immediate to verify that for the reference blade signals are obtained for $i = 1$ and $i = 6$. Then, in the second step, the loads are shifted in Θ consistently with the circumferential shift of the $i - blade$ with respect to the reference one.

Each load can be expressed as the sum of two contributions, the inertial part and the hydrodynamic one: for the aims of this paper, only the hydrodynamic loads will be discussed, since they are more affected by the manoeuvring which gives rise to the large unbalances on the propeller.

4. Results

The results correspondent to the straight ahead motion at $F_N = 0.34$ are discussed in terms of blade loads and the resultant propeller loads (hub loads). The blade loads are discussed in relation to the wake of the twin screw model considered in the previous works [3,4], with the aim to synthesize the cause–and–effect relation between the loads and the inflow to the propeller by a phenomenological perspective. The two models are characterized by similar block coefficient, and in particular, stern appendage configuration; moreover, the propeller sense of revolution is inward from the top in both cases. The assumption of the similarity of the two wakes will be also supported by the character of hub loads, as shown in section 4.2. The loads are presented in terms of ratio with factors $\rho N^2 D^4$ and $\rho N^2 D^5$, for forces and moments, respectively.

4.1. Blade Loads

In table 2 the blade loads are summarized in terms of mean value, r.m.s and its percentage with respect to the mean, and extreme values during the cycle. It has to be observed that

the percentage value of the r.m.s. with respect to the mean is less than 5% for all the loads with the exception of the spindle torque K_{Mz} (less than 10%); the quality of the measure for K_{Mz} is satisfactory considering the small size of the blades and, obviously, the smaller distance of the centre of pressure from the z_B axis, compared to the arms of thrust and tangential force that are relative to the propeller axis.

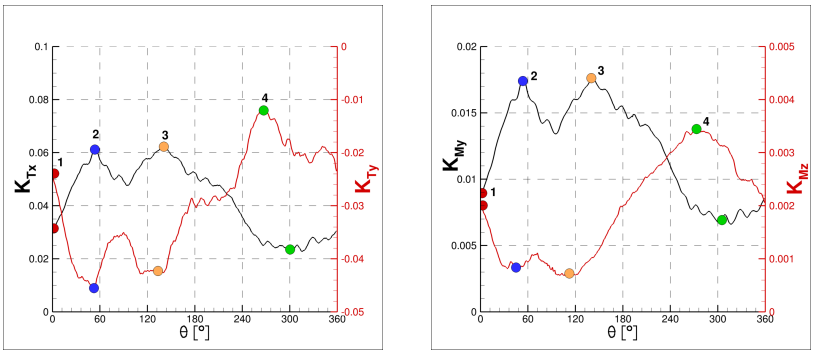

(a) blade thrust and tangential force (b) splindle torque and bending moment

Figure 4. Single blade loads and moments - BLADE frame of reference

Table 2. Blade loads in straight motion

	$\bar{val}$	$\bar{\sigma}$	%	Max	Min
$F_X(\bar{N})$	4.29e-02	1.77e-03	4.1	6.39e-02	2.10e-02
$F_Y(\bar{N})$	-2.97e-02	1.52e-03	5.1	-4.77e-02	-1.03e-02
$M_X(\bar{N}m)$	9.68e-03	3.33e-04	3.4	1.39e-02	5.03e-03
$M_Y(\bar{N}m)$	1.24e-02	4.86e-04	3.9	1.80e-02	6.30e-03
$M_Z(\bar{N}m)$	1.94e-03	1.66e-04	8.5	3.56e-03	4.17e-04

The variation of the blade loads (averaged trend considering more than 200 cycles) are shown in figure 4 in terms of thrust, tangential force, bending and spindle moments. The trend of these loads are discussed considering their relation with the nominal wake at four representative blade angles (identified with colored dots in figure 4), specifically at $\theta = 0°, 60°, 130°$ and $300°$, see figure 5. The nominal wake is visualized in terms of axial velocity (contour lines) and tangential velocity (vectors). The inflow to the propeller is perturbed in the upper half of the disk, the velocity defect being stronger past the two astern brackets; the wake of the forward bracket seems to not affect the inflow, the flow being higher in the sector about $\theta = 0°$. The flow is almost undisturbed in the lower half of the disk. Moreover, it can be observed a non–negligible tangential flow that is upwards oriented. These characteristics are similar for twin screw ships and qualitatively similar features were also observed in [5].

As a consequence of the non–uniform inflow, the blade loads show relatively large fluctuations that correspond to about 40% with respect to the mean value (see also the excursion of the extreme values reported in table 2). Following the blade during the revolution, the loads increase because the blade gradually moves from the region of higher axial speed at ($\theta = 0°$) (point 1, see figure 5a) to that perturbed by the wake of the bracket

and achieve a first maximum at $\theta = 60°$ (point 2, see figure 5b). Then, the loads experience a second peak with magnitude similar to the previous one at $\theta = 130°$; this secondary peak can be associated to the large tangential flow relative to the blade sections, that contributes to increase the angle of incidence and counteracts the opposite effect related to the increase of the axial flow, see figure 5c. This results is qualitatively similar to the measurements showed in [5]. Observing the layout of the figure, it is interesting to observe that the actual circumferential position of the peaks depends also by the skew of the blade, that makes the different blade sections to experience the inflow at staggered, effective locations. Moreover, the phase shift between the peaks of thrust and tangential force (and analogously, bending and spindle moments) might be partially imparted to this effect. During the rotation in the lowest half of the disk the blade is unloaded because the axial flow is not perturbed; the loads reach a minimum about $\theta = 300°$ (point 3), the tangential flow being concurrent to the blade rotation and, therefore, acting to reduce the local incidence of the blade foils, see figure 5d. Then, loads increase due to axial flow reduction caused by the wake of the external astern bracket. It is interesting to observe that the phase shift between the bending moment and the spindle torque is qualitatively similar to that between the thrust and tangential force.

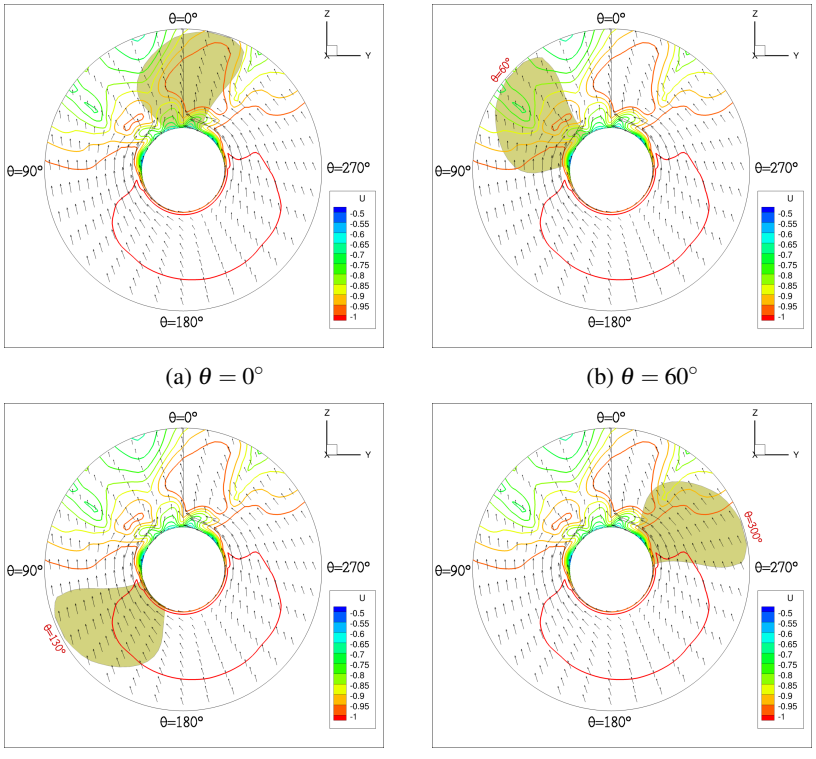

(a) $\theta = 0°$ (b) $\theta = 60°$

(c) $\theta = 130°$ (d) $\theta = 300°$

Figure 5. Inflow encountered by the blade

This is due to the fact that tangential force also provides a non negligible contribution to the spindle torque. K_{M_z} is positive, i.e. it acts to reduce the geometric pitch of the

blade; alternatively, the point of application of the load lies at negative y_b. In fact, the loads tend to be applied in the outer radii of the blade, where the sections are swept back the blade vertical axis.

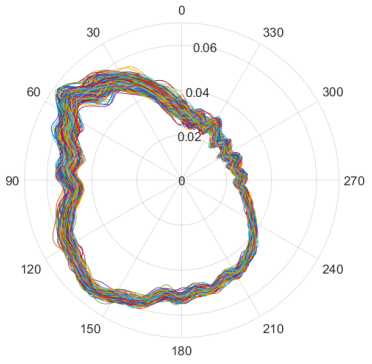

Figure 6. Single blade thrust evolution

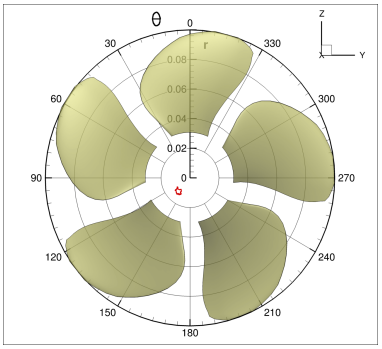

Figure 7. eccentricity

4.2. Propeller Loads

The propeller loads are obtained from the blade loads by the method described in section 3 and are summarized in table 3. It has to be observed that the magnitude of the in–plane forces is similar to the results obtained for the twin screw model investigated in [1]. In particular, the lateral force is negligible and the vertical force, markedly higher, amounts to about 15% of the thrust. This analogy further support the similarity of the wake for the two models and the qualitative reliability of the analysis presented above.

The analysis of the blade forces converted in the hub frame of reference (figure 8) allows to inspect the origin of the in–plane loads and moments developed by the propeller. The side force is outward oriented (negative), because the side force developed by the blade in the upper half of the disk (in particular for $0^\circ < \theta < 90^\circ$ is slightly higher with respect to the lower half. On the contrary, the vertical force K_{T_z} is non–negligible with respect to thrust. In fact, the vertical force (positive) developed by the blade for $0^\circ < \theta < 180^\circ$ is higher with respect to the (negative) one developed in the second half of the cycle, see the trend of the red solid line in figure 8. The propeller in–plane moments can be explained considering the non–homogeneous distribution of the thrust as shown in figure 6. In particular, the blade experience an higher pitching moment in the lower half of the disk, as it can be immediately also deduced by the larger absolute value of the peak at $\theta = 180^\circ$ with respect to that at $\theta = 60^\circ$. Consequently, this moment is negative. This results also support the conclusions about the spindle moment, i.e., the unloading of the blade is associated to the shift of the action point to larger radii. The yaw moment K_{M_z} is negative, because the blade experiences the higher load for $0^\circ < \theta < 180^\circ$ due to higher velocity defect and tangential flow opposite to the blade motion.

5. Conclusions

In this work, a preliminary analysis of blade loads measurements for a free running twin screw model sailing in straight ahead motion was presented. The single blade loads and

Table 3. Propeller loads in straight motion

K_{Tx}	K_{Ty}	K_{Tz}	K_{Mx}	K_{My}	K_{Mz}
2.14e-01	-2.99e-03	3.49e-02	4.83e-02	-9.98e-03	-9.72e-03

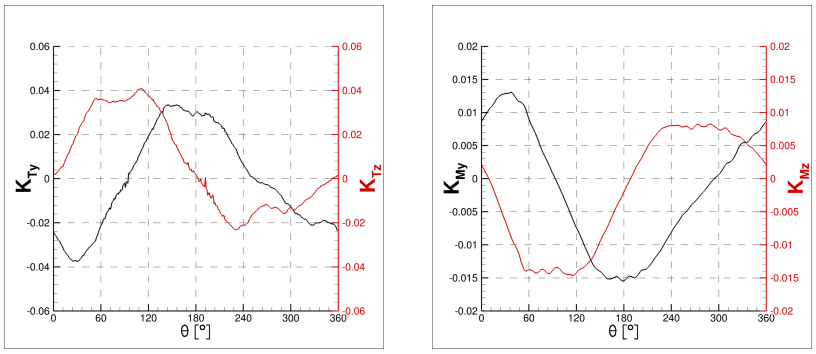

(a) in–plane loads (b) in–plane moments

Figure 8. Single blade loads and moments - HUB frame of reference

the resultant hub propeller loads were presented and discussed in relation to a typical wake developed past a twin screw ship. The measurements, analyzed statistically for more than 100 cycles, showed a low standard deviation with respect to the mean value; the r.m.s. of all the loads was less than 5% with the exception of the r.m.s. of the spindle torque that resulted less than 10%. These preliminary results confirm the reliability of the developed set-up for a fully appended, self-propelled model and, therefore, its use for towing tank experiments too and for acquiring high quality data for the validation of CFD solvers. An in depth statistical and harmonic analysis of these data in maneuvering condition for the complete reliability assessment of the set–up is ongoing.

References

[1] F. Ortolani, S. Mauro, and G. Dubbioso. Investigation of the radial bearing force developed during actual ship operations. part 1: Straight ahead sailing and turning maneuvers. *Ocean Engineering*, 94:67 – 87, 2015.

[2] F. Ortolani, S. Mauro, and G. Dubbioso. Investigation of the radial bearing force developed during actual ship operations. part 2: Unsteady maneuvers. *Ocean Engineering*, 106:424 – 445, 2015.

[3] G. Dubbioso, R. Muscari, F. Ortolani, and A. Di Mascio. Analysis of propeller bearing loads by CFD. Part I: Straight ahead and steady turning maneuvers. *Ocean Engineering*, 130:241–259, 2017.

[4] R. Muscari, G. Dubbioso, F. Ortolani, and A. Di Mascio. Analysis of propeller bearing loads by CFD. Part II: Transient maneuvers. *Ocean Engineering*, 146:217–233, 2017.

[5] S. Jessup, R. Boswell, and J.J. Nelka. Experimental unsteady and time averaged loads of the cp propeller on a model of the dd963 class destroyer for simulated modes of operations. Technical Report No. 77-0110, David Taylor Naval Ship Research and Development Center (DTNSRWDC), 1977.